

## Expression and Modulation of the Intermediate-Conductance $\text{Ca}^{2+}$ -Activated $\text{K}^+$ Channel in Glioblastoma GL-15 Cells

Bernard Fioretti, <sup>a</sup>Emilia Castigli, Maria R. Micheli, <sup>b</sup>Rodolfo Bova, Miriam Sciacaluga, <sup>c</sup>Alexander Harper, Fabio Franciolini and Luigi Catacuzzeno

Dipartimento di Biologia Cellulare e Ambientale, Università di Perugia, <sup>a</sup>CEMIN, Centro di Eccellenza "Materiali Innovativi Nanostrutturati", Università di Perugia, <sup>b</sup>Dipartimento di Medicina Sperimentale e Scienze Biochimiche, Università di Perugia, <sup>c</sup>Division of Molecular Physiology, School of Life Sciences, University of Dundee

### Key Words

Intermediate-conductance  $\text{Ca}^{2+}$ -activated  $\text{K}^+$  channels  
• Human glioblastoma GL-15 cell line • ERK • Cell differentiation • GFAP

### Abstract

We report here the expression and properties of the intermediate-conductance  $\text{Ca}^{2+}$ -activated  $\text{K}^+$  ( $\text{IK}_{\text{Ca}}$ ) channel in the GL-15 human glioblastoma cell line. Macroscopic  $\text{IK}_{\text{Ca}}$  currents on GL-15 cells displayed a mean amplitude of  $7.2 \pm 0.8$  pA/pF at 0 mV, at day 1 after plating. The current was inhibited by clotrimazole (CTL,  $\text{IC}_{50} = 257$  nM), TRAM-34 ( $\text{IC}_{50} = 55$  nM), and charybdotoxin (CTX,  $\text{IC}_{50} = 10.3$  nM). RT-PCR analysis demonstrated the expression of mRNA encoding the  $\text{IK}_{\text{Ca}}$  channel in GL-15 cells. Unitary currents recorded using the inside-out configuration had a con-

ductance of 25 pS, a  $K_D$  for  $\text{Ca}^{2+}$  of 188 nM at -100 mV, and no voltage dependence. We tested whether the  $\text{IK}_{\text{Ca}}$  channel expression in GL-15 cells could be the result of an increased ERK activity. Inhibition of the ERK pathway with the MEK antagonist PD98059 (25  $\mu\text{M}$ , for 5 days) virtually suppressed the  $\text{IK}_{\text{Ca}}$  current in GL-15 cells. PD98059 treatment also increased the length of cellular processes and up-regulated the astrocytic differentiative marker GFAP. A significant reduction of the  $\text{IK}_{\text{Ca}}$  current amplitude was also observed with time in culture, with mean currents of  $7.17 \pm 0.75$  pA/pF at 1-2 days, and  $3.11 \pm 1.35$  pA/pF at 5-6 days after plating. This time-dependent down-regulation of the  $\text{IK}_{\text{Ca}}$  current was not accompanied by changes in the ERK activity, as assessed by immunoblot analysis. Semiquantitative RT-PCR analysis demonstrated a ~35% reduction of the  $\text{IK}_{\text{Ca}}$  channel mRNA resulting from ERK inhibition and a ~50% reduction with time in culture.

Copyright © 2006 S. Karger AG, Basel

## Introduction

The intermediate-conductance  $\text{Ca}^{2+}$ -activated  $\text{K}^+$  ( $\text{IK}_{\text{Ca}}$ ) channel, also known as  $\text{K}_{\text{Ca}}$  3.1,  $\text{IK1}$ ,  $\text{SK4}$ ,  $\text{KCNN4}$ , is a member of the  $\text{Ca}^{2+}$ -activated  $\text{K}^+$  channel family, with a unitary conductance of 20-60 pS in symmetrical 150 mM  $\text{K}^+$  [1-3]. It is distinguished from the functionally related  $\text{Ca}^{2+}$ -activated  $\text{BK}_{\text{Ca}}$  and  $\text{SK}_{\text{Ca}}$  channels of larger (100-200 pS) and smaller (2-20 pS) unitary conductance by its pharmacology, biophysics and physiology. The  $\text{IK}_{\text{Ca}}$  channel is blocked by the scorpion venom toxin CTX, as well as by the antimycotic CTL and its analogue TRAM-34 [4-7]. It is resistant to iberiotoxin, TEA, *d*-tubocurarine, apamin, and scyllatoxin, effective blockers of either  $\text{BK}_{\text{Ca}}$  or  $\text{SK}_{\text{Ca}}$  channels [3, 8, 9]. The recent cloning of the human  $\text{IK}_{\text{Ca}}$  channel has allowed a detailed mapping of its expression in various tissues. The  $\text{IK}_{\text{Ca}}$  channel is chiefly present in peripheral tissues, including secretory epithelia, blood cells and endothelia [1, 10-16]. By linking changes in intracellular  $\text{Ca}^{2+}$  to membrane potential,  $\text{IK}_{\text{Ca}}$  channels are important modulators of several cellular responses relevant to cell transformation, such as progression through the cell cycle, cell growth, differentiation, and volume control [17, 18]. Indeed,  $\text{IK}_{\text{Ca}}$  channels have been found in a variety of transformed cells, such as melanoma, carcinoma, and leukemia [19-21], and in some cases its activity has been found to be involved in cell proliferation [18, 20]. Electrophysiological evidence for the presence of the  $\text{IK}_{\text{Ca}}$  channel has also been provided for the C6 rat glioma cell line [22, 23]. Here we report the expression of the  $\text{IK}_{\text{Ca}}$  channel in the human glioblastoma GL-15 and U-251 cell lines, both exhibiting a poorly differentiated astrocytic phenotype [24-26], and show its modulation by the ERK (extracellular signal-regulated kinase) pathway. The ERKs constitute a family of highly conserved and ubiquitously expressed serine/threonine kinases that are critical components of signalling pathways activated downstream to growth factor receptors or G-protein-linked receptors [27].

The Ras/Raf/MEK/ERK pathway is involved in the control of growth signals, cell survival and invasion, crucial aspects of oncogenic transformation and behaviour. Elevated ERK phosphorylation has been reported in a number of astrocytic tumor cells [28]. The constitutively active ERK seems to originate from mutation or overexpression of growth factor receptors, or to the establishment of autocrine loops originating from overproduction of growth factors such as EGF, FGF, CNTF and PDGF [29]. The Ras/Raf/MEK/ERK pathway is known

to up-regulate the expression of the  $\text{IK}_{\text{Ca}}$  channel, and pharmacological inhibition of the ERK pathway by PD98059, inhibitor of MEK activation, reduced the functional expression of  $\text{IK}_{\text{Ca}}$  channels in fibroblast and endothelial cells [30, 31]. In the present study we tested whether the  $\text{IK}_{\text{Ca}}$  channel was modulated by the ERK pathway, and whether its expression in GL-15 cell line reflects the constitutive activity of this pathway. Pharmacological inhibition of the ERK pathway by PD98059 markedly reduced the  $\text{IK}_{\text{Ca}}$  current, suggesting that this transduction pathway may contribute to the expression of this current in the glioblastoma GL-15 cell line. In agreement with a previous report on human keratinocytes, we found a downregulation of  $\text{IK}_{\text{Ca}}$  channels with time in culture [32]. This down-regulation was not accompanied by changes in ERK activity, and was concomitant with an increase of the differentiation marker glial fibrillary acidic protein (GFAP).

## Materials and Methods

### *Cell cultures*

The glioblastoma GL-15 cell line was grown in minimum essential medium (MEM) supplemented with 10% heat-inactivated foetal bovine serum (FBS), 100 IU/ml penicillin G, 100  $\mu\text{g}/\text{ml}$  streptomycin, and 1 mM sodium pyruvate. The GL-15 cell line, was generated from a human glioblastoma multiforme by Virginia Bocchini (University Medical School, Perugia, Italy; [33]). The human U-251 cell line (astrocytoma type IV) was grown in Dulbecco modified minimum essential medium (DMEM) supplemented with 10% FBS, 100 IU/ml penicillin, and 100  $\mu\text{g}/\text{ml}$  streptomycin. The flasks were incubated at 37°C in a 5%  $\text{CO}_2$  humidified atmosphere. The medium was changed twice weekly and the cells were subcultivated when confluent. For experimental purposes, cells were seeded in Petri dishes at  $100 \times 10^3$  cells/ml and electrophysiological recordings were carried out between 1 and 6 days after seeding. GL-15 cells were treated, one day after trypsinization, with 25  $\mu\text{M}$  PD98059 (in DMSO 0.2%) in culture medium for the indicated time (either 1 or 5 days). Controls for PD98059 were carried out in DMSO 0.2%. Morphological analysis of the cells was performed using a phase contrast Nikon microscope. Cell counts were performed after trypsinization using a Burkert camera.

### *Proliferation assay*

$^3\text{H}$ thymidine incorporation into the DNA was performed by incubating the cells in the various experimental conditions with 1  $\mu\text{Ci}/\text{ml}$   $^3\text{H}$  thymidine (SA 24 Ci/mmol, Amersham) for 2 hours, followed by washing with PBS and fixation with methanol. After 3 washes with 10% TCA, the pellet was solubilized with 0.5 M NaOH and 1% SDS, and counted in a liquid scintillation spectrometer (Beckman).

### Electrophysiology

Macroscopic  $I_{K_{Ca}}$  currents were recorded using the perforated-patch configuration, and activated by coapplication of the  $SK_{Ca}/IK_{Ca}$  activator EBIO (1 mM) and ionomycin (500 nM) (EBIO/ionomycin), in the presence of 3 mM TEA to block the  $BK_{Ca}$  current. Pharmacological characterization studies have demonstrated that the  $SK_{Ca}$  current was absent from the two cell lines used in this study, thus the EBIO/ionomycin-activated current, in the presence of 3 mM TEA, could be taken entirely as  $IK_{Ca}$  current (*cf.* Figure 1). Unitary currents, recorded in inside-out configuration, were activated by elevating the  $[Ca^{2+}]_i$  at the internal side of the membrane. The free  $[Ca^{2+}]_i$  was established by using the software WEBMAXC v2.2. Currents were amplified with a List EPC-7 amplifier (List Medical, Darmstadt, Germany), and digitized with a 12 bit A/D converter (TL-1, DMA interface; Axon Instruments Inc., Foster City, CA, USA). The pClamp software package (version 7.0; Axon Instruments Inc.) was used. For on-line data collection, macroscopic and single-channel currents were filtered at 5 and 0.5 kHz, and sampled at 20 and 200  $\mu$ s/point, respectively. Membrane capacitance measurements were made by using the Membrane Test routine of the pClamp software.

### Solutions and drugs

For whole-cell perforated-patch recordings the bathing Physiological Salt Solution (PSS) consisted of (in mM): NaCl 106.5, KCl 5,  $CaCl_2$  2,  $MgCl_2$  2, MOPS 5, glucose 20, Na-Gluconate 30, octanol 1 (to block gap-junctions; [34, 35]), at pH 7.25, and the pipette solution was:  $K_2SO_4$  57.5, KCl 55,  $MgCl_2$  5, MOPS 10, at pH 7.2. Electrical access to the cytoplasm was achieved by adding amphotericin B (200  $\mu$ M) to the pipette solution. The final access resistances were within the range 10-20 M $\Omega$ . For single-channel inside-out recordings the bathing solution was: KCl (NaCl) 150, EGTA-K (EGTA-Na) 1, MOPS 5,  $MgCl_2$  1, at pH 7.2, and the pipette solution was: KCl 150,  $MgCl_2$  2, MOPS 5, EGTA-K 1, at pH 7.2.  $CaCl_2$  was added in varying amount to obtain the indicated  $[Ca]_i$ . All chemicals used were of analytical grade. Dimethyl sulfoxide (DMSO), TEA, d-TC, and CTL were from Sigma Chemical Co (St. Louis, MO, USA). CTX was from Alomone Labs (Jerusalem, Israel). Ionomycin and EBIO (1-ethyl-2-benzimidazolinone) were from Tocris Cookson Ltd. (Bristol, UK). Stock solutions were obtained by dissolving CTL, EBIO, ionomycin and amphotericin B in DMSO to concentrations of 20, 100, 1 and 500 mM respectively. Pharmacological agents were prepared daily in the appropriate solution at the concentrations stated, and were bath applied by gravity-fed superfusion at a flow rate of 2 ml/min, with complete solution exchange within the recording chamber in around 1 min. The maximal DMSO concentration in the recording solution was about 1%. Experiments were carried out at room temperature (18-22°C). Data are presented as mean $\pm$ SE.

### Indirect immunofluorescence

Cells were extensively washed with phosphate-buffered saline (PBS), immersed in cold methanol, kept at -20°C for 7 minutes, and dried in air. The cells were then incubated for 60 min at room temperature with a rabbit anti-GFAP (Dakopatts,

Denmark) polyclonal antibody (diluted 1:300 in PBS containing 0.3% bovine serum albumin), and then washed in PBS. After treatment with tetramethylrhodamin isothiocyanate (TRITC, Sigma) conjugated goat anti-rabbit IgG (diluted 1:200 in PBS containing 0.3% bovine serum albumin), and washing 3 times with PBS containing 0.1% Tween 20 and twice with PBS alone, preparations were incubated with 2  $\mu$ g/ml DAPI (4,6-diamidino-2-phenylindole) (Sigma) for 5 minutes and dried in air. The preparations were observed with DMRB Leica microscope.

### SDS-polyacrylamide gel electrophoresis and immunoblotting

GL-15 cell cultures were washed with PBS and scraped with 62.5 mM Tris-HCl (pH 6.8), 2 mM ethylenediaminetetraacetic acid (EDTA), 0.5% Triton X-100, phosphatase inhibitor cocktail (Sigma), protease inhibitor cocktail (Sigma) 0.1% SDS. The proteins were separated by SDS-PAGE in 10% acrylamide gel by the Laemmli method [36], then transferred to nitrocellulose filters according to [37]. Immunolabeling of phosphorylated and total-ERKs was performed following the manufacturer directions. The primary antibodies were a mouse anti-phospho-p44/42 MAPK (Thr202/Tyr204) E10 monoclonal antibody, and a rabbit anti-p44/42 MAPK antibody, respectively (Cell Signaling Technologies). The secondary antibodies used to detect phospho- and total ERK content were the peroxidase-conjugated goat anti-mouse immunoglobulins, and the peroxidase-conjugated goat anti-rabbit immunoglobulins (PIERCE). Immunolabeling of GFAP, vimentin, and  $\beta$ -actin were performed by using the anti-GFAP polyclonal antibody (Dakopatts), the anti-vimentin monoclonal antibody (ROCHE), and the anti  $\beta$ -actin monoclonal antibody (Sigma), respectively. The Enhanced Chemiluminescence detection was performed by following the directions of ECL<sup>TM</sup> Western Blotting (Cell Signaling Technologies).

### RT-PCR

Total RNA was extracted using the TRIzol reagent (Gibco BRL) according to the manufacturer instructions, denatured at 70°C for 5 minutes and then reverse transcribed at 37°C for 1 hour in a reaction volume of 50  $\mu$ l containing 20 U of human placental RNase inhibitor (Amersham Biosciences), 1 mM each dNTP (Amersham Biosciences), 4  $\mu$ M random hexamer primers (Amersham Biosciences), 300 U of M-MLV reverse transcriptase (Gibco BRL) in 1x reaction buffer, 4 mM dithiothreitol. PCR was performed using puReTaq Ready-To-Go PCR Beads (Amersham Biosciences) in a total volume of 25  $\mu$ l containing 50 ng cDNA and 0.25  $\mu$ M each primer. PCR primers were: (forward) 5'-GAGAGGCAGGCTGTTAATGC-3' and (reverse) 5'-TGAGACTTCTCGGAGT-3'. These oligonucleotides prime the amplification of a 326 bp fragment [38]. Reaction mixtures were incubated in a PTC100 thermocycler (MJ Research, Inc.) programmed as follows: [1 x (96°C x 5 min)] + [35 x (94°C x 30 sec) (58°C x 1 min) (72°C x 1 min)]. Amplification products were resolved on a 1.5% agarose gel (Bio-Rad) and visualized by ethidium bromide staining.

**Fig. 1.**  $I_{K_{Ca}}$  currents are expressed in human glioblastoma GL-15 cell line. A) Time course of the  $I_{K_{Ca}}$  current activated by EBIO (1 mM) and ionomycin (500 nM) (EBIO/ionomycin), and its block by TRAM-34 (1  $\mu$ M). Individual data points in the current trace represent the  $I_{K_{Ca}}$  current in control condition and following activation by EBIO/ionomycin. The  $I_{K_{Ca}}$  current was assessed at 0 mV using the voltage ramp protocol from -100 to +50 mV, 800 ms duration, from a holding potential of 0 mV, as illustrated in panel B). The bathing solution for the ramp experiments was PSS plus TEA (3 mM), and the pipette solution had 170 mM  $K^+$  as main salt. C) Dose-response relationships for the inhibition of the EBIO/ionomycin-activated current by CTX ( $n=3$ ), CTL ( $n=3$ ), and TRAM-34 ( $n=3$ ). The solid lines represent the best fit of the experimental data with the Hill relationship  $I_{Drug}/I_{CTRL}=1/(1+([Drug]/IC_{50})^{n_H})$ , where  $I_{Drug}$  and  $I_{CTRL}$  are the current in the presence of the given blocker concentration and in control conditions, respectively,  $[Drug]$  is the concentration of the blocker,  $IC_{50}$  is the concentration needed for half-maximal inhibition, and  $n_H$  is the Hill coefficient. The best fit parameters were as follows: CTX,  $IC_{50}=10.3$  nM,  $n_H=1.1$ ; CTL,  $IC_{50}=257$  nM,  $n_H=0.85$ ; TRAM-34,  $IC_{50}=55$  nM,  $n_H=0.83$ . Experimental conditions and protocol were as in panel A). D) RT-PCR analysis of  $I_{K_{Ca}}$  expression in GL-15 and U-251 cells. Lane 2,  $\phi$ X174-*HaeIII* m.w. marker; lanes 1 and 3, 326 bp amplification product obtained from GL-15 and U-251 cells, respectively, using  $I_{K_{Ca}}$  specific primers.

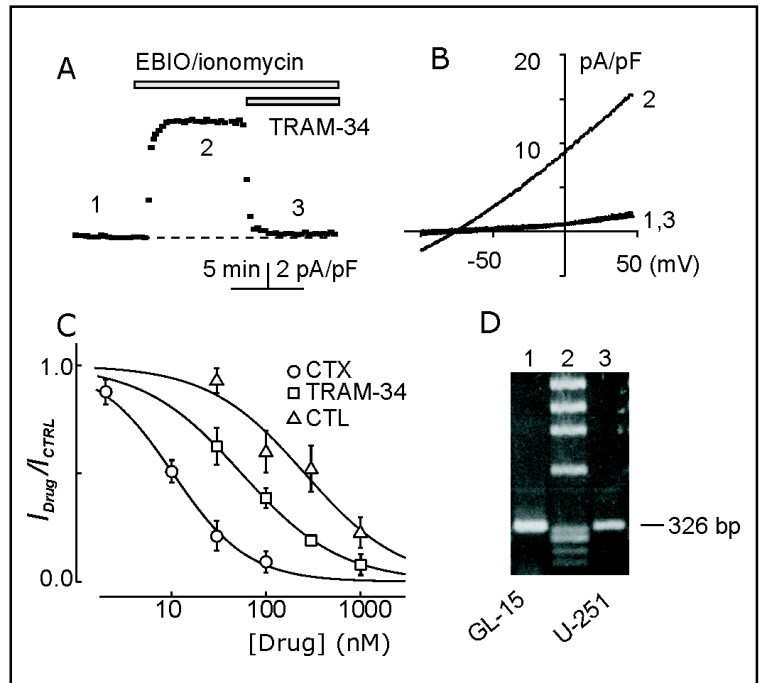
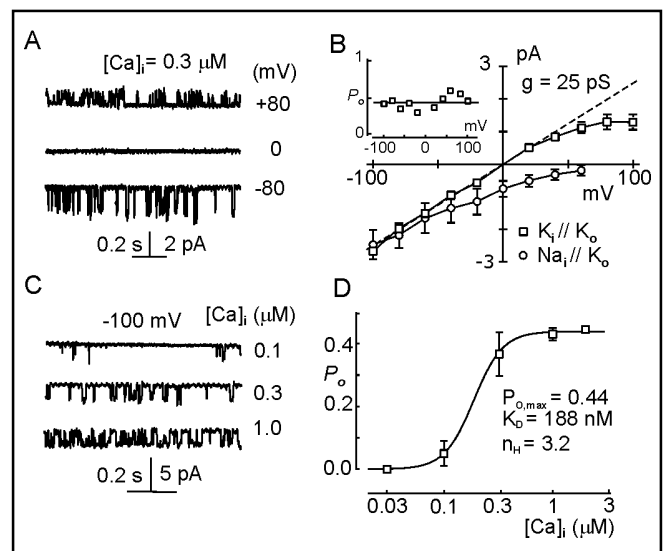


**Fig. 2.** Unitary  $I_{K_{Ca}}$  current properties from the human glioblastoma GL-15 cell line. A) Representative inside-out single channel recordings obtained at the indicated voltages, in symmetrical 150 mM  $K^+$  solutions, and with 0.3  $\mu$ M  $[Ca]_i$  at the cytoplasmic side of the patch. External solution contained 3 mM TEA. B) Unitary  $I-V$  relationships obtained from three inside-out patches in symmetrical 150 mM  $K^+$  (squares), and after substitution of the internal  $K^+$  with  $Na^+$  (circles). The dashed line, representing the linear fit of the control data points at negative voltages, gives a slope conductance of 25 pS. Inset: Plot of the  $I_{K_{Ca}}$  channel  $P_o$  vs. voltage for the patch shown in panel A). C) Representative inside-out single channel recordings obtained at -100 mV in symmetrical 150 mM  $K^+$  solutions, at the indicated  $[Ca]_i$ . External solution contained 3 mM TEA. D) Plot of the  $I_{K_{Ca}}$  channel  $P_o$  vs.  $[Ca]_i$  obtained from three inside-out patches in symmetrical 150 mM  $K^+$ , at -100 mV, similar to that shown in panel C). The solid line represents the best fit of the experimental data with a Hill relationship of the form  $P_o = P_{o,max} / [1 + (K_D / [Ca^{2+}]_i)^{n_H}]$ . The best fit parameters were  $P_{o,max}=0.44$ ,  $K_D=188$  nM and  $n_H=3.2$ .

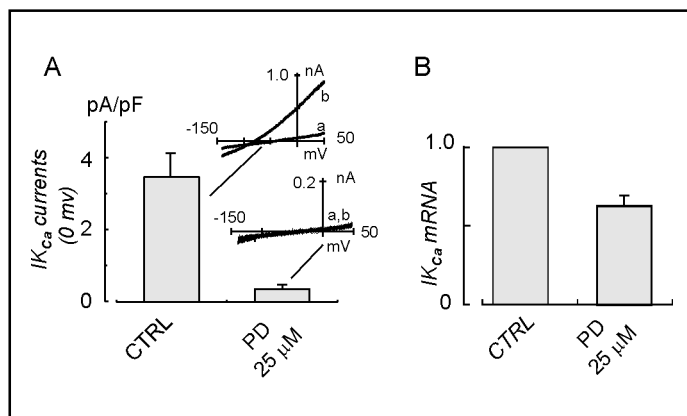


#### Semiquantitative RT-PCR

Quantitation of target RNA level in different samples was performed through coamplification (in the same test tube) with the constitutively expressed  $\beta$ -actin RNA as an endogenous control. Trial experiments were performed in order to determine the optimal range of cycle number allowing product detection within the linear phase of amplification. According to the results of such experiments,  $\beta$ -actin specific primers were added

10 cycles after the beginning of  $I_{K_{Ca}}$  cDNA amplification and the reaction was stopped after a total of 34 cycles. The following  $\beta$ -actin specific primers were used: (forward) 5'-TGA CGG GGT CAC CCA CAC TGT GCC CATC TA-3' and (reverse) 5'-CTA GAAG CATT TGC GTG GAC GAT GGAG GG-3'. These oligonucleotides prime the amplification of a 661 bp fragment (NM\_001101). Ethidium bromide stained gels were photographed under UV light with Polaroid type 665 films and

**Fig. 3.** Modulation of  $IK_{Ca}$  currents by PD98059 in human glioblastoma GL-15 cell line. A) Mean  $IK_{Ca}$  current density assessed at day 5 in control conditions, and following 5-days treatment with PD98059 (25  $\mu$ M). Inset: Representative current ramps (from -140 to +50 mV, from a holding potential of 0 mV) in control conditions and in PD98059, before (a) and after (b) application of EBIO (1 mM) and ionomycin (500 nM). The bathing solution was PSS plus 3 mM TEA, the pipette solution had 170 mM  $K^+$  as main salt. B)  $IK_{Ca}$  mRNA levels in control cells and in cells pretreated with PD98059 (25  $\mu$ M, 5 days). The mean of four independent semiquantitative RT-PCR assays  $\pm$ SE is presented.  $IK_{Ca}$  mRNA levels detected in PD98059-treated cells were normalized to the levels detected in control cells.



quantitation was performed by densitometric analysis of scanned Polaroid negatives using the freeware NIH-Image. Data were obtained as a ratio of the signal of target PCR product to the signal of  $\beta$ -actin PCR product. The  $IK_{Ca}$  mRNA levels detected in PD98059-treated cells were then normalized to the levels detected in control cells.

#### Measurements of cell cycle by flow cytometry

Aliquots of cell suspensions subjected to different treatments were washed with PBS (400xg, 7 min) and processed for the cell cycle analysis by propidium iodide (PI)-staining and flow cytometry. Briefly, the cell pellet was resuspended in 0.5 ml of hypotonic fluorochrome solution (50  $\mu$ g/ml PI in 0.1% sodium citrate plus 0.1% Triton X-100) in 12x75mm polypropylene tubes (Becton and Dickinson, Lincoln Park, NJ, USA). The tubes were kept at 4°C for at least 30 min before flow cytometric analysis. The PI fluorescence of individual nuclei was measured using a FACScan flow cytometer (Becton Dickinson, Mountain View, CA, USA) at wavelength of 488 nm. The percentages of the cells in G0/G1, S and G2/M phases were calculated using CellFIT Cell-Cycle Analysis Version 2.0.2. Software.

## Results

### The glioblastoma GL-15 human cell line expresses $IK_{Ca}$ currents

Several human glioma cell lines have been reported to express  $BK_{Ca}$  channels [39], and it is now becoming apparent that their expression is a common feature of glioma cells. By contrast, to our knowledge few studies have investigated the expression of other  $K_{Ca}$  conductances in glioma cell lines. We used a standard patch clamp electrophysiological approach to test for the presence of, and characterize the properties of  $IK_{Ca}$  and  $SK_{Ca}$  channels in the GL-15 cell line model. These experiments were performed in the presence of 3 mM TEA in the bath to prevent any potential contamination by the  $BK_{Ca}$

current. Co-application of the  $SK_{Ca}/IK_{Ca}$  channel activator EBIO (1 mM; [40]) and ionomycin (0.5  $\mu$ M) (EBIO/ionomycin) evoked a stable outward K current. A typical experiment illustrating the action of EBIO/ionomycin on GL-15 cells recorded using the perforated-patch configuration is presented in Figure 1A (also *cf.* [35]). Individual data points in the current trace depict the outward current recorded in control conditions (1) and following application of EBIO/ionomycin (2) and TRAM-34, 1  $\mu$ M (3), assessed at 0 mV using the voltage ramp protocol presented in Figure 1B. The mean outward current following EBIO/ionomycin application was  $7.2 \pm 0.8$  pA/pF, at day 1 after plating ( $n=10$ ). The sensitivity of the EBIO/ionomycin-activated current to TRAM-34 identifies it as an  $IK_{Ca}$  current. The mean reversal potential determined with the voltage ramp protocol was  $-83 \pm 3$  mV ( $n=3$ ), a value close to the  $K^+$  equilibrium potential for the recording conditions used ( $E_K = -90$  mV, calculated from the Nernst relationship). Further support for the EBIO/ionomycin-activated current being an  $IK_{Ca}$  current was provided by its pharmacological profile matching that of an  $IK_{Ca}$  current (Figure 1C). CTX, CTL, and TRAM-34 inhibited the EBIO/ionomycin-activated current with  $IC_{50}$  of 10.3 nM, 257 nM, and 55 nM, respectively, values well in agreement with other native and cloned  $IK_{Ca}$  channels (see Introduction). *d*-TC (100  $\mu$ M), a specific blocker of the  $SK_{Ca}$  channel did not affect the EBIO/ionomycin-activated current (data not shown). RT-PCR analysis performed on both human glioblastoma GL-15 and U-251 cell lines demonstrated the expression of the  $IK_{Ca}$  mRNA (Figure 1D).

We then used inside-out isolated patch recordings to investigate the biophysical properties of the  $IK_{Ca}$  channel. Unitary currents were commonly observed with symmetrical 150 mM  $K^+$ , and a  $Ca^{2+}$  concentration greater than 0.1  $\mu$ M at the inner side of the membrane (Figure

2A, C). The  $I$ - $V$  relationship constructed using a double gaussian fit of the current amplitude histograms revealed a significant inward rectification, and a mean single-channel conductance (assessed by a linear fit of the  $I$ - $V$  data at negative voltages) of  $25 \pm 3$  pS ( $n=7$ ; Figure 2B). The  $IK_{Ca}$  channel was highly selective for  $K^+$  vs.  $Na^+$ . With 150  $Na^+$  inside and 150  $K^+$  outside, the  $P_{Na^+}/P_{K^+}$  was  $<0.096$ , as estimated from the GHK relationship, based on the observation that at +60 mV the current was still inward (Figure 2B, circle). We also assessed the voltage dependence of the  $IK_{Ca}$  channel activity. In agreement with previous reports  $IK_{Ca}$  channel was insensitive to voltage (see Inset to Figure 2B which plots the channel open probability,  $P_o$ , as function of voltage, derived from the experiment shown in panel A). The  $Ca^{2+}$ -sensitivity of the channel was assessed using inside-out patches in symmetrical 150 mM  $K^+$  and holding potential of -100 mV (Figure 2C). The plot in panel D shows the  $P_o$  data at various  $[Ca^{2+}]_i$ , from three patches. Data points were well fitted by a Hill isotherm with  $P_{0,max}=0.44$ ,  $K_D=188$  nM, and  $n_H=3.2$ .  $IK_{Ca}$  currents displaying similar electrophysiological and pharmacological properties were also found in another human glioma cell line, the U-251 (data not shown).

#### Modulation of the $IK_{Ca}$ channel expression

In several non-transformed cells,  $IK_{Ca}$  channel expression has been shown to be modulated by signals originating from growth factor receptor activation, such as the ERK pathway [30, 31]. We used the MEK antagonist PD98059, an inhibitor of ERK (ERK1/2) activation to test whether  $IK_{Ca}$  channel expression in glioblastoma GL-15 cells is linked to the ERK pathway. One day after plating, cells were incubated for five days with PD98059 (25  $\mu$ M). The  $IK_{Ca}$  current was assessed from voltage ramps as the EBIO/ionomycin-activated current, in the presence of external 3 mM TEA (cf. Figure 3A, inset). The mean  $IK_{Ca}$  current recorded from PD98059-treated cells was  $0.37 \pm 0.10$  pA/pF ( $n=21$ ), a value considerably lower than that recorded from control cells ( $3.5 \pm 1.3$  pA/pF;  $n=15$ , Figure 3A). Moreover, acute application of 25  $\mu$ M PD98059 did not significantly affect the EBIO/ionomycin-activated current, indicating that the  $IK$  channel is not directly inhibited by PD98059 ( $n=4$ , data not shown). A semiquantitative RT-PCR analysis was performed to verify whether the downregulation of the  $IK_{Ca}$  current with PD98059 treatment resulted from modulation of transcription. Following treatment with PD98059, the level of  $IK_{Ca}$  mRNA was found to be reduced by 36%, compared to non-treated cells. The data from four

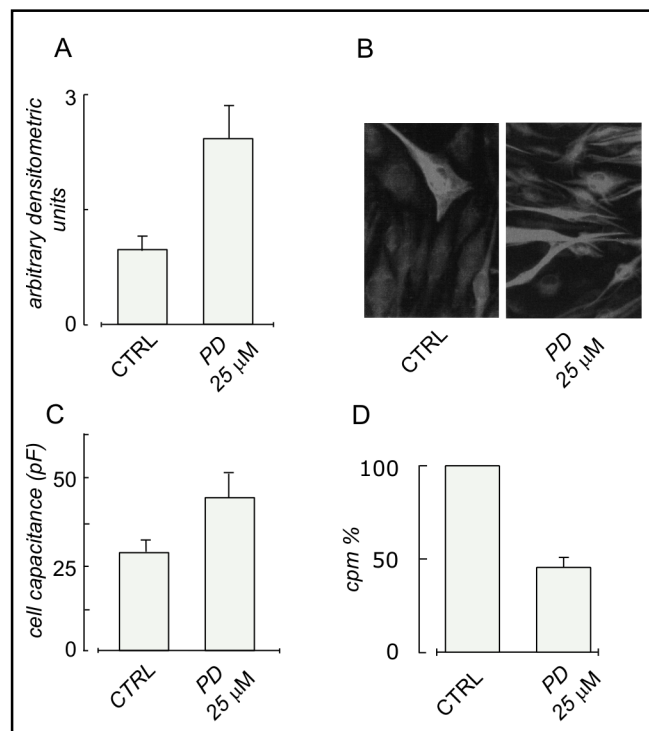
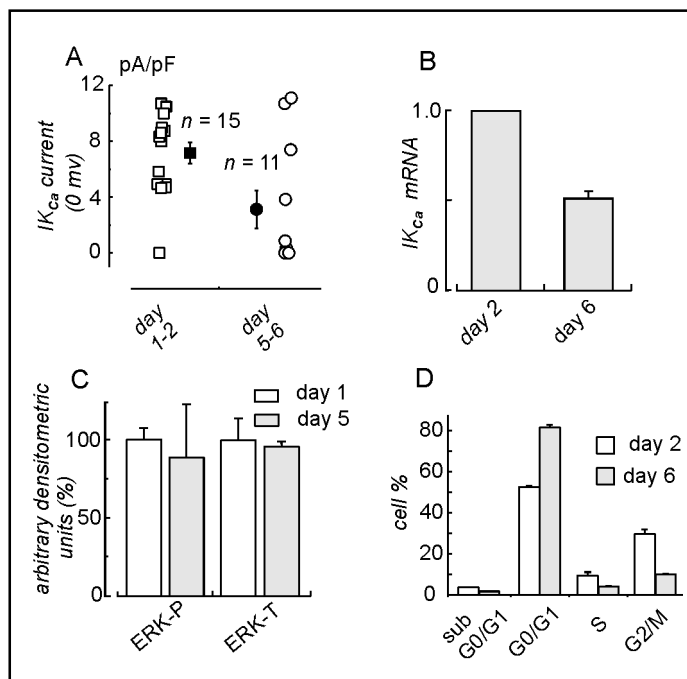


**Fig. 4.** Cellular effects of PD98059 in human glioblastoma GL-15 cell line. A) GFAP expression in cultured GL-15 cells grown for 5 days either in control conditions, or in presence of PD98059 (25  $\mu$ M), assessed by immunoblotting analysis (see Methods). B) Immunofluorescence staining of GFAP expression carried out on cultured GL-15 cells grown for 5 days either in control conditions (left), or in presence of PD98059 (25  $\mu$ M, right). C) Mean membrane capacitance of GL-15 cells grown for 5 days either in control conditions, or in presence of 25  $\mu$ M of PD98059. D) Plots of [ $^3H$ ]thymidine incorporation on cultured GL-15 cells grown for 1 day either in control conditions, or in presence of 25  $\mu$ M of PD98059 (see Methods).

independent RT-PCR experiments are summarized in the bar histogram of Figure 3B.

We have shown that PD98059 effectively abolishes the  $IK_{Ca}$  current in GL-15 cells. Other findings indicate that PD98059 treatment makes GL-15 cells take on a more differentiated phenotype. PD98059 increased the expression of the differentiated astrocytic marker GFAP (assessed by immunoblot analysis, Figure 4A). At the single-cell level, the GFAP was present in a small fraction of control cells (Figure 4B, left), similar to the pattern for many high grade gliomas [41]. Following PD98059 treatment most cells displayed positive immunoreactivity to GFAP (Figure 4B, right), as is the case of normal, differentiated astrocytes. In addition, PD98059-treated cells displayed longer processes compared to control cells, in

**Fig. 5.** Modulation of  $I_{K_{Ca}}$  currents by time in culture. A) Dispersion plot of  $I_{K_{Ca}}$  current density activated by EBIO/ionomycin, under perforated patch configuration, from actively proliferating cells (at day 1-2 after plating;  $n=15$ ), and from confluent cells (at day 5-6 after plating;  $n=11$ ). The mean  $I_{K_{Ca}}$  current of each data set is shown as a filled symbol. The bathing solution was PSS plus 3 mM TEA, and the pipette solution had 170 mM  $K^+$  as main salt. B)  $I_{K_{Ca}}$  mRNA levels in GL-15 cells at day 2 and day 6 after plating. The mean of five independent semiquantitative RT-PCR assays  $\pm$  SE is presented.  $I_{K_{Ca}}$  mRNA levels detected at day 6 were normalized to the levels detected at day 2. C) Densitometric analysis of immunoblotting data of phosphorylated (Thr202/Tyr204) and total ERKs at day 1 and at day 5 after plating, expressed as percent of the value at day 1. Data were normalized with the anti- $\beta$ -actin antibody. D) Analysis of cell cycle evaluated by PI staining and flow cytometry at day 2 and at day 6 after plating.



accordance with the increase observed in cell capacitance (Figure 4C). In agreement with these findings, PD98059 inhibits cell division, as assessed from cell counts (data not shown), and [ $^3$ H]thymidine incorporation (Figure 4D). Interestingly the intermediate filament vimentin, highly expressed in GL-15 cells [24] but absent in mature astrocytes, was unaffected by PD98059, indicating that the expression of this protein is not under the ERK pathway regulation (data not shown). This result indicates that other biochemical pathways participate to the overall regulation of the transformed phenotype.

$I_{K_{Ca}}$  channels seem to be downregulated also by time of subculturing, decreasing by 57% in four days (1-2 days:  $7.1 \pm 0.7$  pA/pF,  $n=15$ ; 5-6 days:  $3.1 \pm 1.3$  pA/pF,  $n=11$ ; Figure 5A). As shown in Figure 5B, semiquantitative RT-PCR analysis demonstrated that the level of  $I_{K_{Ca}}$  mRNA is nearly halved at day 6 after plating, compared to control cells (day 2). During this time period (i.e., from day 1-2 to day 5-6), the morphology of GL-15 cells underwent changes similar to those observed following PD98059 treatment. The time of subculturing also induced a marked increase of GFAP expression (as already reported by Moretto et al. [42]), while both vimentin and  $\beta$ -actin levels were not affected (data not shown). These findings are similar to those reported by Langlois et al. [43] who analysed the expression of cytoskeletal proteins in U343 MG-A astrocytoma cells following the induction of a differentiated phenotype.

We then tested whether the time-dependent downregulation of the  $I_{K_{Ca}}$  could be secondary to an inhibition of ERK activity resulting from contact inhibitory signals released from cells that had reached confluence. The ERK activity in control (day 1) and confluent (day 5) GL-15 cells was assessed by using specific antibodies against the double phosphorylated (Thr202/Tyr204) and total ERKs, respectively. A quantitative analysis of the immunoblotting data, obtained by anti- $\beta$ -actin antibody normalization, is shown in Figure 5C. No change of ERK activity was observed with time of subculturing indicating that the  $I_{K_{Ca}}$  current in GL-15 cells is also regulated by an ERK-independent pathway.

Another possible interpretation of our data is that the  $I_{K_{Ca}}$  channel downregulation is associated with the exit of the cells from the cycle (i.e., G0 phase), an occurrence shown to modulate the expression of cell cycle-dependent genes. To verify this possibility we performed cell cycle analysis on GL-15 cells at day 2 and 6 of subculturing. The results illustrated in Figure 5D show a significant increase (ca. 1.6 fold) in the percentage of cells in the G0/G1 phase at day 6 of subculturing, compared to day 2, suggesting a significant increase in the number of cells that exit the cycle. This view is also supported by data on GFAP, a marker of cell differentiation (i.e., of cells in the G0 phase), that has been shown to increase with time in GL-15 cells [42].

## Discussion

### *The human glioblastoma GL-15 cell line expresses the $IK_{Ca}$ channel*

In this study we report the expression and modulation of the  $IK_{Ca}$  channel in human glioblastoma cell lines. The identification of the  $IK_{Ca}$  channel was based on pharmacological and biophysical properties assessed both at the macroscopic and unitary current level. The properties of the  $IK_{Ca}$  channel, such as  $Ca^{2+}$ - and voltage-dependence, unitary conductance and sensitivity to inhibitors fit with those reported for cloned  $IK_{Ca}$  channels [2, 3, 9]. The finding of the transcript for the  $IK_{Ca}$  channel confirms identification. The  $IK_{Ca}$  channel was found to be highly expressed in the glioblastoma cell line studied here, its current density amounting to 7.2 pA/pF ( $n=10$ , at day 1).  $IK_{Ca}$  currents with properties similar to those found in GL-15 cells were also found in the human glioma cell line U-251 (this study) and in the C6 rat glioma cell line [22]. Expression of  $IK_{Ca}$  channels may be a signature of glioma cell lines since this channel is not (or very scantily) expressed in normal human brain [2, 3, 9]. Other ion channels have been reported to display an altered expression in glioblastoma cells. Reduced expression of inward rectifier  $K^+$  channels [44], increased expression of amiloride-sensitive  $Na^+$  channels [45], voltage-activated  $Cl$  channels [46], and  $BK_{Ca}$  channels [39] have in fact been reported in several gliomas, compared to normal astrocytes. The human glioblastoma GL-15 and U-251 cell lines exhibit a poorly differentiated astrocytic phenotype [25, 26]. Interestingly, GL-15 cells have been shown to be tumorigenic *in vivo*, and to display the invasiveness potential typical of glioblastomas [47]. Moreover, along with genomic alterations typical of glioblastomas [33], GL-15 cells express high levels of vimentin [33] and nestin (our unpublished data). This cell line thus seems to mirror the behaviour of specific sub-populations of glioblastoma cells that display some properties of astrocyte-restricted precursor cells [48].

### *Modulation of the $IK_{Ca}$ channels*

Another finding of this study is that the  $IK_{Ca}$  channel expression is under dual, ERK-dependent and independent modulation. We found that the ERK pathway inhibitor PD98059 dramatically reduced the  $IK_{Ca}$  current (Figure 3A), placing the ERK pathway in a central position with regard to  $IK_{Ca}$  channel expression in the GL-15 cell line. The Ras/Raf/MEK/ERK pathway is involved in the control of growth signals, cell survival and invasion, crucial aspects of oncogenic transformation and behav-

our. Gliomas and glioblastomas are known to accumulate genomic alterations leading to abnormal activation of signal transduction pathways involved in the control of Ras activity, with the result that the downstream effector ERK may be constitutively active. Thus, a working hypothesis is that the sustained ERK activity is partly responsible for the expression of the  $IK_{Ca}$  channels in GL-15 cells. Since a sustained ERK activity is found in several transformed cells [28], our findings raise the possibility that the expression of  $IK_{Ca}$  channel may be a rather common feature among transformed cells. Indeed,  $IK_{Ca}$  channels have been found in a variety of transformed cells, such as melanoma, carcinoma, and leukemia [19, 20, 35].

Several mechanisms might, in principle, underlie the ERK-dependent  $IK_{Ca}$  current modulation, such as regulation of  $IK_{Ca}$  channel expression and/or post-translational channel regulation. The possibility that the  $IK_{Ca}$  current inhibition observed in PD98059-treated cells is due to a downregulation of the  $IK_{Ca}$  mRNA levels was investigated by semiquantitative RT-PCR analysis. Our results showed that a significant reduction of  $IK_{Ca}$  mRNA occurred following PD98059 treatment. However, the observed reduction of ~35% is, apparently, not large enough to account for such a strong inhibitory effect of PD98059 on the  $IK_{Ca}$  current, thus indicating that an additional mechanism is possibly involved. Further investigation is required to elucidate these aspects. A recent report suggests that an inhibition of  $IK_{Ca}$  mRNA translation could be implicated [49]. These authors demonstrated that a contribution of the Ras pathway to glioblastoma development is to be ascribed mainly to its effects on translational efficiency (recruitment of specific mRNAs to ribosomes), rather than transcription of specific genes. Interestingly, protein mislocation has been recently taken to explain the paradox of lack of functional expression of inward rectifier currents, in spite of the presence of its mRNA in glioma models [44]. This explanation could be used to interpret our data. The  $IK_{Ca}$  current has also been found to decrease with time of subculturing (Figure 5A). The signalling pathway involved in this time-dependent downregulation is not known, but the data reported here seem to exclude that it is secondary to a time-dependent downregulation of the ERK activity. Similar to the  $IK_{Ca}$  channel downregulation resulting from ERK inhibition, the time-dependent  $IK_{Ca}$  channel downregulation is associated with a marked increase of GFAP expression, marker of mature astrocytes. These results seem to suggest that the  $IK_{Ca}$  channel expression is subject to the same (differentiation) signals controlling GFAP expression. Moreo-



ver, a number of studies report that  $IK_{Ca}$  channels are downregulated during differentiation in tumor and normal models (C6 rat glioma cells [23]; the keratinocyte cell line HaCaT [32]; myogenic cell lines [50, 51]; promyelocytes during granulocytic differentiation [21]), although in few cases an upregulation of the  $IK_{Ca}$  channel expression has been observed following differentiation [52, 53].

In this study we report the expression and modulation of the  $IK_{Ca}$  channel in two human glioblastoma cell lines. This channel is considered to be important in several cellular responses involved in cell transformation, such as progression through the cell cycle, cell growth, differ-

entiation, and volume regulation. An understanding of which specific mechanism(s) and function(s) this channel underpins in glioblastoma cells is therefore of much interest.

## Acknowledgements

We are grateful to Dr Heike Wulff for the generous gift of TRAM-34, and Dr Rosario Donato for kindly providing the U-251 cell line. This work was supported by a grant from the Fondazione Cassa Risparmio Perugia.

## References

- Logsdon NJ, Kang J, Togo JA, Christian EP, Aiyar J: A novel gene, hKCa4, encodes the calcium-activated potassium channel in human T lymphocytes. *Biol Chem* 1997;272:32723-6.
- Joiner WJ, Wang LY, Tang MD, Kaczmarek LK: hSK4, a member of a novel subfamily of calcium-activated potassium channels. *Proc Natl Acad Sci USA* 1997;94:11013-8.
- Ishii TM, Silvia C, Hirschberg B, Bond CT, Adelman JP, Maylie J: A human intermediate conductance calcium activated potassium channel. *Proc Natl Acad Sci USA* 1997;94:11651-6.
- Wulff H, Miller MJ, Hansel W, Grissmer S, Cahalan MD, Chandy KG: Design of a potent and selective inhibitor of the intermediate-conductance  $Ca^{2+}$ -activated  $K^{+}$  channel, IKCa1: a potential immunosuppressant. *Proc Natl Acad Sci U S A* 2000;97:8151-6.
- Mauler F, Hinz V, Horvath E, Schuhmacher J, Hofmann HA, Wirtz S, Hahn MG, Urbahns K: Selective intermediate-/small-conductance calcium-activated potassium channel (KCNN4) blockers are potent and effective therapeutics in experimental brain oedema and traumatic brain injury caused by acute subdural haematoma. *Eur J Neurosci* 2004;20:1761-8.
- Narenjkar J, Assem el- SK, Ganellin CR: Inhibition of the antigen-induced activation of RBL-2H3 cells by cetiedil and some of its analogues. *Eur J Pharmacol* 2004;483:107-16.
- Chandy KG, Wulff H, Beeton C, Pennington M, Gutman GA, Cahalan MD:  $K^{+}$  channels as targets for specific immunomodulation. *Trends Pharmacol Sci* 2004;25:280-9.
- Vergara C, Latorre R, Marrion NV, Adelman JP: Calcium-activated potassium channels. *Curr Opin Neurobiol* 1998;8:321-9.
- Jensen BS, Strobaek D, Christophersen P, Jorgensen TD, Hansen C, Silahtaroglu A, Olesen SP, Ahning PK: Characterization of the cloned human intermediate-conductance  $Ca^{2+}$ -activated  $K^{+}$  channel. *Am J Physiol* 1998;275:C848-56.
- Rufo PA, Merlin D, Riegler M, Ferguson-Maltzman MH, Dickinson BL, Brugnara C, Alper SL, Lencer WI: The antifungal antibiotic, clotrimazole, inhibits chloride secretion by human intestinal T84 cells via blockade of distinct basolateral  $K^{+}$  conductances. Demonstration of efficacy in intact rabbit colon and in an in vivo mouse model of cholera. *J Clin Invest* 1997;100:3111-20.
- Begenisich T, Nakamoto T, Ovitt CE, Nehrke K, C. Brugnara, S.L. Alper, J.E. Melvin, Physiological roles of the intermediate conductance,  $Ca^{2+}$ -activated potassium channel Kcnn4. *J Biol Chem* 2004, 279:47681-7.
- Ghanshani S, Wulff H, Miller MJ, Rohm H, Neben A, Gutman GA, Cahalan MD, Chandy KG: Up-regulation of the IKCa1 potassium channel during T-cell activation. Molecular mechanism and functional consequences. *J Biol Chem* 2000;275:37137-49.
- Kohler R, Wulff R, Eichler I, Kneifel M, Neumann D, Knorr A, Grgic I, Kampfe D, Si H, Wibawa J, Real R, Borner K, Brakemeier S, Orzechowski HD, Reusch HP, Paul M, Chandy KG, Hoyer J: Blockade of the intermediate-conductance calcium-activated potassium channel as a new therapeutic strategy for restenosis. *Circulation* 2003;108:1119-25.
- Schilling T, Stock C, Schwab A, Eder C: Functional importance of  $Ca^{2+}$ -activated  $K^{+}$  channels for lysophosphatidic acid-induced microglial migration. *Eur J Neurosci* 2004;19:1469-74.
- Ayabe T, Wulff H, Darmoul D, Cahalan MD, Chandy KG, Ouellette AJ: Modulation of mouse Paneth cell alpha-defensin secretion by mIKCa1, a  $Ca^{2+}$ -activated, intermediate conductance potassium channel. *J Biol Chem* 2002;277:3793-800.
- Chen MX, Gorman SA, Benson B, Singh K, Hieble JP, Michel MC, Tate SN, Trezise DJ: Small and intermediate conductance  $Ca^{2+}$ -activated  $K^{+}$  channels confer distinctive patterns of distribution in human tissues and differential cellular localisation in the colon and corpus cavernosum. *Naunyn Schmiedeberg's Arch Pharmacol* 2004;369:602-15.
- Wang Z: Roles of  $K^{+}$  channels in regulating tumour cell proliferation and apoptosis. *Pflugers Arch* 2004;448:274-86.
- Ouadid-Ahidouch H, Roudbaraki M, Delcourt P, Ahidouch A, Joury N, Prevarskaya N: Functional and molecular identification of intermediate conductance  $Ca^{2+}$ -activated  $K^{+}$  channels in breast cancer cells: association with cell cycle progression. *Am J Physiol Cell Physiol* 2004;287:125-34.
- Meyer R, Schonherr R, Gavrilova-Ruch O, Wohlrab W, Heinemann SH: Identification of ether a go-go and calcium-activated potassium channels in human melanoma cells. *J Membr Biol* 1999;171:107-15.

- 20 Jager H, Dreker T, Buck A, Giehl K, Gress T, Grissmer S: Blockage of intermediate-conductance  $Ca^{2+}$ -activated  $K^+$  channels inhibit human pancreatic cancer cell growth in vitro. *Mol Pharmacol* 2004;65:630-8.
- 21 Wieland SJ, Gong QH, Chou RH, Brent LH: A lineage-specific  $Ca^{2+}$ -activated  $K^+$  conductance in HL-60 cells. *J Biol Chem* 1992;267:15426-31.
- 22 Manor D, Moran N: Modulation of small conductance calcium-activated potassium channels in C6 glioma cells. *Membr Biol* 1994;140:69-79.
- 23 Kuo TC, Lin-Shiau SY: Decrease in  $Ca^{2+}$ -activated  $K^+$  conductance in differentiated C6-glioma cells. *Neurochem Res* 2004;29:1453-9.
- 24 Bocchini V, Beccari T, Arcuri C, Bruyere L, Fages C, Tardy M: Glial fibrillary acidic protein and its encoding mRNA exhibit mosaic expression in a glioblastoma multiform cell line of clonal origin. *Int J Dev Neurosci* 1993;11:485-92.
- 25 Tlhyama T, Lee VM, Trojanowski JQ: Co-expression of low molecular weight neurofilament protein and glial fibrillary acidic protein in established human glioma cell lines. *Am J Pathol* 1993;142:883-92.
- 26 Castigli E, Arcuri C, Giovagnoli L, Luciani R, Giovagnoli L, Secca T, Gianfranceschi GL, Bocchini V: Interleukin-1 $\alpha$  induces apoptosis in GL15 glioblastoma-derived human cell line. *Am J Physiol* 2000;279:2043-9.
- 27 Pearson G, Robinson F, Beers Gibson T, Xu BE, Karandikar M, Berman K, Cobb MH: Mitogen-Activated Protein (MAP) kinase pathways: regulation and physiological functions. *Endocr Reviews* 2001;22:153-83.
- 28 Mandell JW, Hussaini IM, Zecevic M, Weber MJ, VandenBerg SR: In situ visualization of intratumor growth factor signaling: immunohistochemical localization of activated ERK/MAP kinase in glial neoplasms. *Am J Pathol* 1998;153:1411-23.
- 29 Holland EC: Gliomagenesis: genetic alterations and mouse models. *Nat Rev Genet* 2001;2:120-9.
- 30 Pena TL, Chen SH, Konieczny SF, Rane SG: Ras/MEK/ERK Up-regulation of the fibroblast  $K_{Ca}$  channel FIK is a common mechanism for basic fibroblast growth factor and transforming growth factor-beta suppression of myogenesis. *J Biol Chem* 2000;275:13677-82.
- 31 Brakemeier S, Kersten A, Eichler I, Grgic I, Zakrzewicz A, Hopp H, Kohler R, Hoyer J: Shear stress-induced up-regulation of the intermediate-conductance  $Ca^{2+}$ -activated  $K^+$  channel in human endothelium. *Cardiovasc Res* 2003;60:488-96.
- 32 Koegel H, Alzheimer C: Expression and biological significance of  $Ca^{2+}$ -activated ion channels in human keratinocytes. *FASEB J* 2001;15:145-154.
- 33 Bocchini V, Casalone R, Collini P, Rebel G, Lo Curto F: Changes in glial fibrillary acidic protein and karyotype during culturing of two cell lines established from human glioblastoma multiforme. *Cell Tissue Res* 1991;265:73-81.
- 34 Eskandari S, Zampighi GA, Leung DW, Wright EM, Loo DD: Inhibition of gap junction hemichannels by chloride channel blockers. *J Membr Biol* 2002;185:93-102.
- 35 Fioretti B, Castigli E, Calzuola I, Harper AA, Franciolini F, Catacuzzeno L: NPPB block of the intermediate-conductance  $Ca^{2+}$ -activated  $K^+$  channel. *Eur J Pharmacol* 2004;497:1-6.
- 36 Laemmli UK: Cleavage of structural proteins during the assembly of the head of bacteriophage T4. *Nature* 1970;227:680-685.
- 37 Towbin H, Staehelin T, Gordon J: Electrophoretic transfer of proteins from polyacrylamide gels to nitrocellulose sheets: procedure and some applications. *Proc Natl Acad Sci USA* 1979;76:4350-4354.
- 38 Kohler R, Degenhardt C, Kuhn M, Runkel N, Paul M, Hoyer J: Expression and function of endothelial  $Ca^{2+}$ -activated  $K^+$  channels in human mesenteric artery: A single-cell reverse transcriptase-polymerase chain reaction and electrophysiological study in situ. *Circ Res* 2000;87:496-503.
- 39 Liu X, Chang Y, Reinhart PH, Sontheimer H, Chang Y: Cloning and characterization of glioma BK, a novel BK channel isoform highly expressed in human glioma cells. *J Neurosci* 2002;22:1840-9.
- 40 Singh S, Syme CA, Singh AK, Devor DC, Bridges RJ: Benzimidazolone activators of chloride secretion: potential therapeutics for cystic fibrosis and chronic obstructive pulmonary disease. *J Pharmacol Exp Ther* 2001;296:600-11.
- 41 Rutka JT, Murakami M, Dirks PB, Hubbard SL, Becker LE, Fukuyama K, Jung S, Tsugu A, Matsuzawa K: Role of glial filaments in cells and tumors of glial origin: a review. *J Neurosurg* 1997;87:420-30.
- 42 Moretto G, Brutti N, De Angelis V, Arcuri C, Bocchini V: A time-dependent increase in glial fibrillary acidic protein expression and glutamine synthetase activity in long-term subculture of the GL15 glioma cell line. *Cell Mol Neurobiol* 1997;17:509-19.
- 43 Langlois A, Lee S, Kim DS, Dirks PB, Rutka JT: p16(ink4a) and retinoic acid modulate rhoA and GFAP expression during induction of a stellate phenotype in U343 MG-A astrocytoma cells. *Glia* 2002;40:85-94.
- 44 Olsen ML, Sontheimer H: Mislocalization of Kir channels in malignant glia. *Glia* 2004;46:63-73.
- 45 Bubien JK, Keeton DA, Fuller CM, Gillespie GY, Reddy AT, Mapstone TB, Benos DJ: Malignant human gliomas express an amiloride-sensitive  $Na^+$  conductance. *Am J Physiol* 1999;276:1405-10.
- 46 Ransom CB, O'Neal JT, Sontheimer H: Volume-activated chloride currents contribute to the resting conductance and invasive migration of human glioma cells. *J Neurosci* 2001;21:7674-83.
- 47 Guillamo JS, Lisovski F, Christov C, Le Guerinel C, Defer GL, Peschanski M, Lefrancois T: Migration pathways of human glioblastoma cells xenografted into the immunosuppressed rat brain. *J Neurooncol* 2001;52:205-15.
- 48 Lee JC, Mayer-Proschel M, Rao MS: Gliogenesis in the central nervous system. *Glia* 2000;30:105-21.
- 49 Rajasekhar VK, Viale A, Socci ND, Wiedmann M, Hu X, Holland EC: Oncogenic Ras and Akt signaling contribute to glioblastoma formation by differential recruitment of existing mRNAs to polysomes. *Mol Cell* 2003;12:889-901.
- 50 Pena TL, Rane SG: The small conductance calcium-activated potassium channel regulates ion channel expression in C3H10T1/2 cells ectopically expressing the muscle regulatory factor MRF4. *J Biol Chem* 1997;272:21909-16.
- 51 Fioretti B, Pietrangelo T, Catacuzzeno L, Franciolini F: Intermediate-conductance  $Ca^{2+}$ -activated  $K^+$  channel is expressed in C2C12 myoblasts and is downregulated during myogenesis. *Am J Physiol Cell Physiol* 2005;289:C89-96.
- 52 Vandorpe DH, Shmukler BE, Jiang L, Lim B, Maylie J, Adelman JP, de Franceschi L, Cappellini MD, Brugnara C, Alper SL: cDNA cloning and functional characterization of the mouse  $Ca^{2+}$ -gated  $K^+$  channel, mK1. Roles in regulatory volume decrease and erythroid differentiation. *J Biol Chem* 1998;273:21542-53.
- 53 Manaves V, Qin W, Bauer AL, Rossie S, Kobayashi M, Rane SG: Calcium and Vitamin D increase mRNA levels for the growth control hK1 channel in human epidermal keratinocytes but functional channels are not observed. *BMC Dermatol* 2004;4:7-19.